Copyright © 2009 by ABCM

NATURAL CONVECTION IN A PARTIALLY OPEN SQUARE CAVITY WITH INTERNAL HEAT SOURCE: ANALYSING THE FLOW

Adriano da Silva, e-mail: adriano@unochapeco.edu.br
Éliton Fontana, e-mail: eliton_fontana@hotmail.com
Adriano Cancelier, e-mail: adrianoc@unochapeco.edu.br
Universidade Comunitária Regional de Chapecó – UNOCHAPECÓ
Rua Senador Atílio Fontana, 591 E, CEP: 89809-000, Chapecó, SC, Brasil
Viviana Cocco Mariani,
Programa de Pós-Graduação em Engenharia Mecânica – PUCPR
Rua Imaculada Conceição, 1155, Prado Velho, CEP: 81611-970, Curitiba, PR, Brasil
e-mail: viviana.mariani@pucpr.br

Abstract. *Steady buoyancy-driven flow of air in a partially open square cavity with internal heat source is investigated numerically in this work. This configuration can be found in many electronics equipment, where the open is designed for increase the cooling of internal components. The study of this case is also relevant in others applications, like the construction and operation of nuclear reactors, solar energy collectors, energy storages systems, indoor design and construction. In this work was analyzed a square 2D enclosure with adiabatic bottom and top walls, and vertical walls maintained in different constant temperatures. A heat source with 1% of the enclosure volume is present in the center of the bottom wall. The right (cold) wall contains a partial open occupying 50% of the total wall size, to allow the entrance and exit of air. The influence of the temperature gradient between the verticals walls was analyzed in the interval for $Ra_e = 10^3$ to 10^5, while the influence of the heat source was availed through the relation $R=Ra_i/Ra_e$, investigated between 400 and 2000. The governing equation system was solved with the CFD code ANSYS CFX, using an 82×82 structured mesh. The code validation was realized comparing some results with data found in literature, showing good agreement. Results are presented for the maximum dimensionless temperature achieved in the enclosure, isotherms, streamlines and air velocity profile in the opening, showing significant influence of the heat source on the mass flow intensity, thermal behavior and fluid dynamics of the air.*

***Keywords**: natural convection, Rayleigh numbers, square cavity, heat source.*

1. INTRODUCTION

In recent decades, the study of natural convection in cavities has been the subject of many works. Natural convection in open cavities and slots are encountered in many engineering applications, such as solar thermal receiver, heat convection from extended surfaces in heat exchangers, solar collectors with insulated strips (Sazia and Mohamad, 1999), etc. Cavities with opening side and internal heat source can be seen in many electronic devices, where the openings facilitate the cooling of apparatus internal components. Furthermore, the study of this case is relevant in many other applications, among which can be cited: construction and operation of nuclear reactors, solar energy collectors, energy storage systems, design and construction of indoor environments, grains storage, among others. Many works are presented in the literature, where it was evaluated the behavior of fluids within the cavities, some are cited below.

The natural convection in cavities induced by the difference of temperature between vertical (or horizontal) walls is a case widely studied (Zitzman *et al.* (2005), Pesso and Piva (2009), Costa (2005), Davis (2005), Abourida *et al.* (1998), Yilbas *et al.*, 1998, Barakos *et al.* (2005)). In those studies, the authors evaluated the influence of the temperature difference, aspect ratio and inclinations of the cavity in the thermal behavior of the fluid contained inside. Michalek (2005) conducted experiments measuring water flow contained in a cubical cavity with isothermal vertical walls and adiabatic horizontal walls for values of Ra_e greater than 10^9. The transition from stationary for non-stationary flow was below the theoretical value of critical Rayleigh number. Bilen and Oztop (2005) performed a numerical study of heat transfer by natural convection in a cavity 2D inclined and partially open. A parametric study was conducted for values of Ra_e between 10^3 and 10^6, concluding that the value of Nu is maximized for angles between 30° and 60° and for low values of Ra_e, while at high values of Ra_e, the value of Nu is maximized for angles between 60° and 90°. Kuznik *et al.* (2007) used Lattice-Boltzmann method with non-uniform mesh for the simulation of natural convection in a square cavity. The authors investigated the transition region between 10^3 and 10^9 for Rayleigh numbers, with good agreement with those reported in the literature. The same method was used by Mezrhab *et al.* (2006), where it was evaluated the influence of the cavity inclination and the existence of an internal partition. There was a maximum reduction in heat transfer for a range of Rayleigh numbers between 6×10^3 and 2×10^4.

When there is an internal source of energy in cavities large changes in the internal flow characteristics happens. Studies on natural convection in cavities with internal heat source can be found in (Kuznetsov and Sheremet (2008), Nakhi and Chamkha (2007), Oztop and Bilgen (2006), Oztop and Abu-Nada (2008)). In many cases, the cavity presents a partial opening, which facilitates mass flow and therefore the cooling process. Mariani and Silva (2007) conducted a numerical study of the thermal and fluid dynamic behavior of air in partially open 2D enclosures based on two aspects of the radius, H/W = 1 and 2. The enclosure had an opening on the right wall and a small heating source located on the bottom or left vertical wall, occupying three different positions. Numerical simulations were performed for Rae in the range between 10^3 and 10^6, it was founded that the parameter modifications have significant effects on the average and local Nusselt numbers of the enclosures. A similar study was done by Kandaswamy *et al.* (2007), where the influence of the position and the size of the heat source were evaluated. That study was conducted for values of Grashof between 10^3 and 10^5.

Hence the present study proposes a study of natural convection in partially open cavity submitted to temperature differences between the left and right walls and an internal heat conduction source. It is evaluated the influence of the internal heat source intensity in the thermal and fluid dynamic behavior of air into of opening cavity, and the inflow mass rate in the opening. Local results are presented in form of streamline and isotherm plots, and local Nusselt numbers over the hot and cold walls providing valuable insight to the physical processes.

2. PHYSICAL DOMAIN AND GOVERNING EQUATIONS

The fluid is investigated in a square cavity with width W and height H heated on the left vertical wall by T_H and cooled on the upper half of the right vertical wall by T_C. The temperature difference is function of Rayleigh numbers. The two vertical walls have a temperature prescribed, while the horizontal walls are adiabatic, the average temperature used was 25^{o}C into the cavity. The two-dimensional computational domain and the Cartesian system of coordinates used here are illustrated in Figure 1. The position W/H = 0.5 illustrated in Figure 1 is the distance considered, for example, from the left hand lateral wall to the center of the heating source. The internal heat source is located on the bottom or left vertical wall at different places and occupies 1% of the total volume of the enclosures. The opening was evaluated for 0.5H. The lower half of the right wall is open and is in contact with the air outside the enclosure. The fluid considered into the cavity is atmospheric air with Prandtl number, Pr = 0.71.

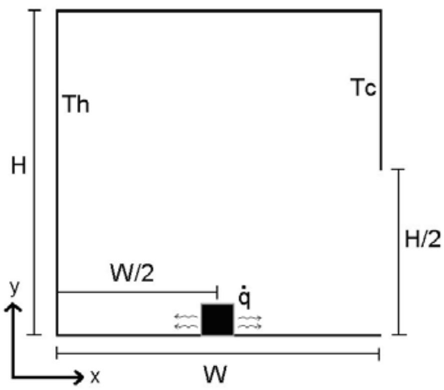

Figure 1: Domain employed.

To model the flow under study, we use the conservation equations for mass, momentum, and energy for two-dimensional, steady and laminar flow. For the moderate temperature difference considered in this work, all the physical properties of the fluid, μ, k, and c_p, are considered constant except the density, in the buoyancy term, which obeys the Boussinesq approximation. In the energy conservation equation, we neglect the effects of compressibility and viscous dissipation. Thus, the equations that govern the flow and heat transfer are:

$$\frac{\partial(\rho u)}{\partial x}+\frac{\partial(\rho v)}{\partial y}=0 \tag{1}$$

$$\frac{\partial(uu)}{\partial x}+\frac{\partial(uv)}{\partial y}=-\frac{1}{\rho}\frac{\partial p}{\partial x}+\frac{\mu}{\rho}\left[\frac{\partial^2 u}{\partial x^2}+\frac{\partial^2 u}{\partial y^2}\right] \tag{2}$$

$$\frac{\partial(uv)}{\partial x}+\frac{\partial(vv)}{\partial y}=-\frac{1}{\rho}\frac{\partial p}{\partial y}+\frac{\mu}{\rho}\left[\frac{\partial^2 v}{\partial x^2}+\frac{\partial^2 v}{\partial y^2}\right]+g\beta(T-T_{ref}) \tag{3}$$

$$\frac{\partial(uT)}{\partial x}+\frac{\partial(vT)}{\partial y}=\alpha\left[\frac{\partial^2 T}{\partial x^2}+\frac{\partial^2 T}{\partial y^2}\right]+\frac{\dot{q}}{\rho c_p} \tag{4}$$

The temperature was evaluated in dimensionless form as,

$$\theta=\frac{T-T_c}{T_H-T_C} \tag{5}$$

where T_C is cold temperature and T_H is hot temperature.

The boundary conditions used are:

$u = v = 0$, and $\theta = 0$ in $x = W;\ H/2 \le y \le H$ (6)

$u = v = 0$, and $\theta = 0$ in $x = W;\ 0 \le y \le H$ (7)

$u = v = 0$, and $\partial\theta/\partial y = 0$ in $0 \le x \le W;\ y = 0$ (8)

$u = v = 0$, and $\partial\theta/\partial y = 0$ in $0 \le x \le W;\ y = H$ (9)

$k_S\, \partial\theta_S/\partial n = k_f\, \partial\theta_f/\partial n$ at the source – fluid interfaces (10)

where the subscript *s* denotes the source and *f* denotes the fluid.

The external Rayleigh number is represented by the difference of temperature between vertical walls, $10^3 \le Ra_e \le 10^5$,

$$Ra_e = \frac{g\beta(T_H - T_C)H^3}{\nu\alpha} \tag{11}$$

and the intensity of heat produced by the source heat is represented by the internal Rayleigh number, Ra_i, which is based on the volumetric heat-generation rate,

$$Ra_i = \frac{g\beta q H^5}{\nu\alpha k} \tag{12}$$

The influence of the intensity of the two Rayleigh numbers is evaluated by means of the relation:

$$R = \frac{Ra_i}{Ra_e} \tag{13}$$

where the values for R are $R = 400$, $R = 1000$ e $R = 2000$.

Other physical quantities of interest in the present study are the local Nusselt numbers along the hot and cold walls. The variables are defined, respectively, as:

$$Nu_H = \left.\frac{\partial\theta}{\partial X}\right|_{X=0} \tag{14}$$

$$Nu_C = \left.\frac{\partial\theta}{\partial X}\right|_{X=W} \tag{15}$$

where $X = x/L$.

The stream function is defined as:

$$u = \frac{\partial\Psi}{\partial Y} \tag{16}$$

$$v = -\frac{\partial\Psi}{\partial X} \tag{17}$$

but the numerical results are presented in terms of the dimensionless stream function given by:

$$\Psi_{\dim} = \frac{\Psi}{\alpha} \tag{18}$$

The air velocity in opening is evaluated by dimensionless velocity defined as:

$$u^* = \frac{u}{u_{\max}} \tag{19}$$

where u_{max} is the maximum velocity for each Rayleigh number used. The velocity is calculated in function of dimensionless height given by:

$$Y^* = \frac{y}{0,5H} \tag{20}$$

The relative maximum velocity, $\overline{u}_{\max}$, gives the relation between the maximum velocity and the maximum velocity for $Ra_e = 10^3$, i.e., $u_{\max}\big|_{10^3}$,

$$\overline{u}_{\max} = \frac{u_{\max}}{u_{\max}\big|_{10^3}} \tag{21}$$

3. NUMERICAL METHODOLY

The numerical solution of the governing equations was performed using the commercial computational fluid dynamics code CFX, version 11. In this code the conservation equations for mass, momentum and energy are solved using the finite volume discretization method generated by an structured mesh. For this practice the solution domain is divided into small control volumes, and the governing differential equations are integrated over each control volume with use of the Gauss theorem. The resulting discrete system of linear equations is solved using an algebraic multigrid methodology called additive correction accelerated incomplete lower upper (ILU) factorization technique (Patankar (1980), Maliska (2004)). It is an iterative solver whereby the exact solution of the equations is approached during the course of several iterations. The solution was considered converged when the sum of absolute normalized residuals for all cells in the flow domain becomes less than 10^{-6}.

The validation of the computer code has been verified for the natural convection problem in a closed square cavity without a heat conduction source. The results for hot or cold average Nusselt ($\overline{Nu} = \int \left(\partial\theta/\partial X\right)\big|_{X=0,\,W} dY$) for two meshes, 42×42 and 82×82, and for two Rayleigh numbers, 10^5 and 10^6, are presented in Table 1. In both cases, Cartesian structured meshes were employed. The numerical results shown in Table 1 are compared with results from Hortmann *et al.* (1990) and Mariani and Silva (2007) presenting mean standard deviation of 2.87% for grid 42×42 and of 0.26% for grid 82×82.

Table 1: Average Nusselt: comparison with literature.

	42 ×42			82 ×82		
	Hortmann (1990)	Mariani and Silva (2007)	Present study	Hortmann (1990)	Mariani and Silva (2007)	Present study
$Ra_e = 10^5$	4.616	4.605	4.776	4.525	4.535	4.545
$Ra_e = 10^6$	9.422	9.487	9.675	8.977	8.975	8.993

Another comparison of numerical results was made using local results in the form of streamline and isotherm plots from Xia and Zhou (1992) for *R* = 2500 and opening of 0.5H, such results are illustrated in Figure 2. Note that numerical results obtained in this study are in good agreement with results of Xia and Zhou (1992).

In order to choice the number of volumes required to obtain a grid independent solution some numerical simulations were made. In fact, five structured computational grid levels were used and more one unstructured grid for the physical domain. The refinement was mainly promoted at the walls of the cavity and next to heat source, where the gradients are higher. The numerical validation was conducted for results of dimensionless maximum temperature for R = 400 and $10^3 \leq Rae \leq 10^5$ as detailed in Table 2.

Table 2: Dimensionless maximum temperature and computing time required for the grid selected in this study.

Grid	32×32	42×42	62×62	82×82	122×122	Unstructured
$Rae = 10^3$	3.532	3.538	3.538	3.538	3.538	3.538
$Rae = 10^4$	2.800	2.830	2.860	2.870	2.870	2.870
$Rae = 10^5$	2.183	2.216	2.293	2.340	2.342	2.345
Dimensionless Time	1	1.43	4.37	6.560	13.55	28.05

The precision of the grids has been analyzed by comparing their predicted results. Besides the accuracy, the computing cost is another important aspect related to the grid's performance. The same table lists the computing dimensionless time, i.e., the relation between CPU time for each grid. From these results, it was then decided by using a structured mesh with 82 x 82 elements, because the use of a more refined mesh not changes the results and demands for several time of resolution, thus the mesh used can be seen in Figure 3.

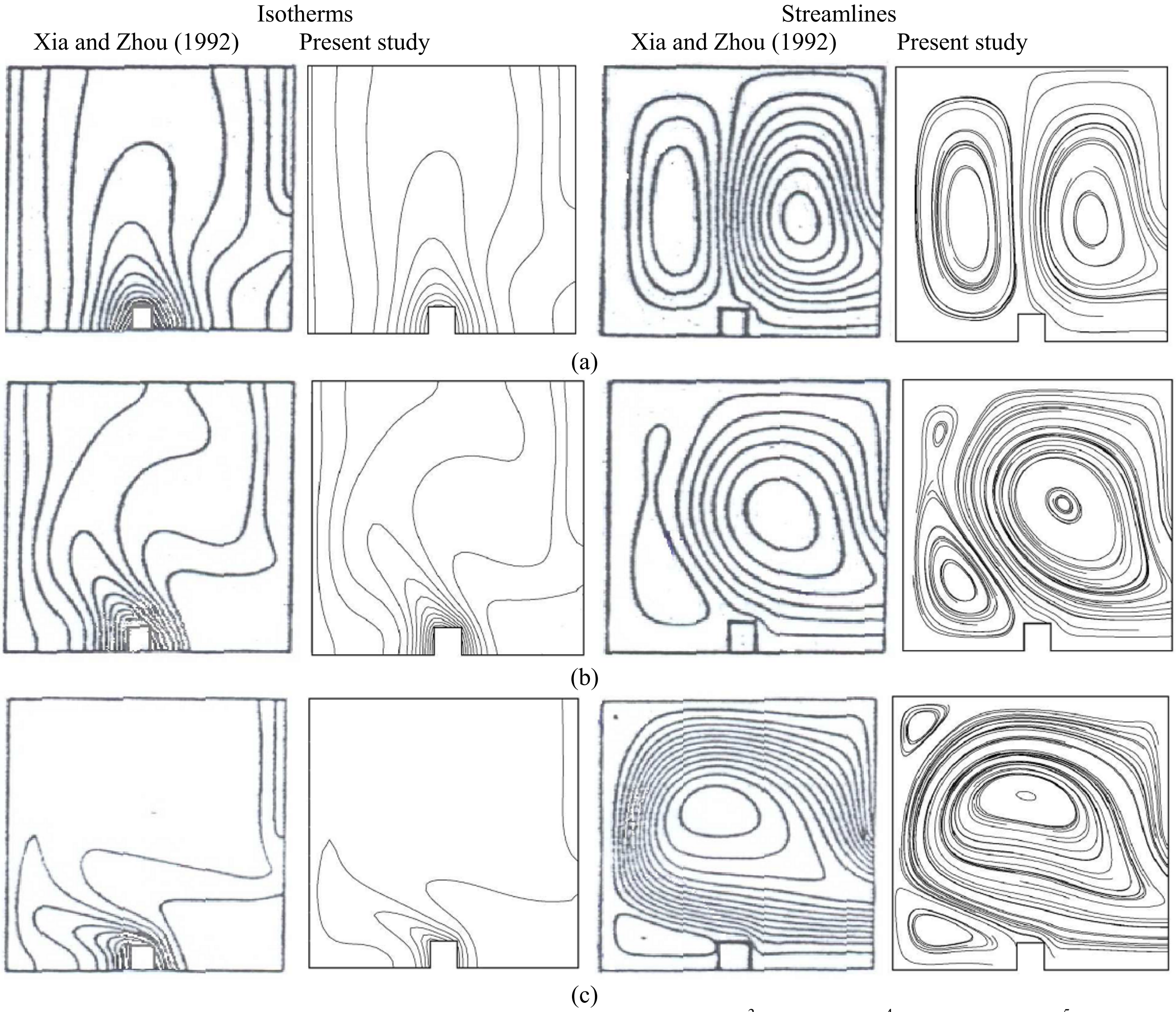

Figure 2: Isotherms and streamlines for R = 2500 and (a) $Ra_e = 10^3$, (b) $Ra_e = 10^4$, and (c) $Ra_e = 10^5$.

4. RESULTS AND DISCUSSION

In some cases the materials contained into the cavity are sensitive to high temperatures, such as electronic components, where the chips may suffer damage if the temperature is too high at some point. Thus, it was determined the maximum temperature reached into the cavity for the different conditions studied, as can be seen in Table 3.

According to Table 3 for all values of R the dimensionless maximum temperature decreases with increasing value of Ra_e, because the air moves with greater velocity into the cavity, facilitating heat exchange. For small values of Ra_e, the air next to heat source is more stagnant, thus increasing its temperature. When the value of R is increasing, there is a considerable increase in the maximum temperature for all values of Ra_e. This occur due to the fact that the maximum temperature is reached in a region next to the heat source, so increasing the influence of heat source with relation the difference of temperature between walls, there are a relative increase temperature in this region.

The streamlines and isotherms for various values of R and Ra_e are presented in Figures 4 and 5, respectively. In Figure 4 analyzing the results for R = 400 note that two circulations there are into the cavity. For $Ra_e = 10^3$ both circulations are significant indicating that the air flow is influenced by the presence of heat source. However, as can be seen, one of circulations is greater, indicating the influence of the temperature difference between the walls. For higher values of Ra_e, the size of the secondary recirculation is lower than the primary, indicating that the flow is dominated by the difference in temperature between the vertical walls.

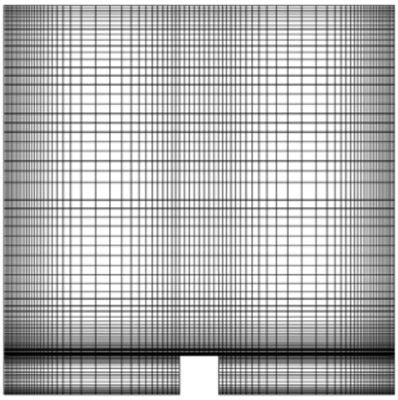

Figure 3: Mesh with 82×82 control volumes.

Table 3: Dimensionless maximum temperature.

R	Ra_e	θ_{max}
400	10^3	3.538
	10^4	2.879
	10^5	2.331
1000	10^3	7.077
	10^4	5.485
	10^5	3.812
2000	10^3	11.50
	10^4	8.138
	10^5	5.643

The flow characteristics influence also the temperature distribution inside the cavity. As can be seen in Figure 5, where R = 400 e $Ra_e = 10^3$, there is the formation of isotherms with characteristic of parables, which indicates that the temperature is distributed in the form of layers around the heat source. This behavior is typical of a system where there is an internal heat source, but without the presence of temperature gradient between the walls. Similar analysis can be made to $Ra_e = 10^4$, but with lower intensity. In order, for $Ra_e = 10^5$ occur the formation of isotherms with characteristic more horizontal. This type of temperature distribution is typical of systems where the convection occurs only due to a temperature gradient between the vertical walls, showing that the heat source has a smaller influence on the isotherms, which is in agreement with the analysis of streamlines plots.

Increasing the value of R, it increases the influence of heat source. A direct reflection of this fact can be seen in the streamlines plot when R = 1000 or R = 2000 and $Ra_e = 10^3$. In these cases, there are two circulations inside the cavity with dimensions comparable, so that the gradient of temperature between vertical walls exerts little influence. This effect can also be seen in the isotherms, where there is a predominance of parabolic isotherms.

For R = 1000 and $Ra_e = 10^4$, note that there are two secondary circulations, with lower dimensions in relation to main circulation. These are formed due to the influence of heat source, but in general the flow is controlled by the temperature difference between the walls. The distribution of temperature, as seen in Figure 5, shows two regions with distinct characteristics. The region closest to the hot wall is influenced mainly by the heat source, while that in region next to opening, the isotherms are more horizontal, thus influenced by the temperature difference between the walls.

The isotherms for R = 2000 and $Ra_e = 10^4$ are quite similar to those found for the same value of Ra_e and R = 1000, with the presence of two regions, one controlled by the heat and another by the difference in temperature between the walls. However, the streamlines obtained for R = 2000 differ in the sense that no occurs the formation of two small circulations almost isolated, but the formation of a circulation of higher intensity, resulting in greater influence from the heat source. For $Ra_e = 10^5$ in all cases studied the flow was controlled by the temperature difference between the walls. For R = 2000 can be seen a small recirculation in the upper left, but well lower to the main circulation.

Figure 6 illustrates the profiles of the dimensionless horizontal velocity in the opening for various R or Ra_e. The maximum relative velocities using with base the value for $Ra_e = 10^3$ are 1, 5.45 and 11.43 for $Ra_e = 10^3$, 10^4 and 10^5, respectively. At a fixed Ra_e, when R increases, the portion of the opening occupied by the inflow becomes slightly smaller, the maximum dimensionless velocity become larger, and the position of the maximum outflow velocity move slightly towards the bottom wall. At a fixed R, the change of the characteristics of the opening with Ra_e is more complicated. In Figure 6 there is a region of inflow at bottom and outflow at top cavity. Null velocity occurs when there is a change in flow direction, such region is next to the center of the opening for $Ra_e = 10^3$, while for $Ra_e = 10^4$ such region appears before of the center of opening, because the point of maximum velocity occurs at bottom of cavity. In both cases the influence of the values of R is significant. The profiles obtained for $Ra_e = 10^5$ (see Figure 6c) show that R has little influence on the outflow or inflow of the cavity, because in this case, as already mentioned above, the process is basically controlled by the temperature difference between the walls. In this case, point of null velocity does not coincide for all values of R, but in all cases the maximum velocity is reached at top of the opening, so that the point of null velocity occurs above the center of the opening.

The values obtained for local Nusselt along the hot and cold walls are shown in Figure 7. It can be seen from Figure 7b that the local Nusselt numbers along the cold wall show similar behavior for all values of R, with a maximum at Y* = 0 and a minimum at Y* = 1. The heat exchange is more intense in the region next to the opening, decreasing rapidly to a value which remains almost constant. The heat exchange is increasing in the region next to the opening because the direction of flow varies and it leaves the cavity. This causes an increasing in velocity gradient in normal direction to the surface, with consequent increasing in local velocity. Note that when R = 400 or R = 1000, the increase in Ra_e values cause an increase in the values of local Nusselt along the cold wall indicating that the intensity of heat exchange in cold wall is influenced by temperature difference between the walls. In fact, looking at the isotherms and streamlines, one can see that for these cases, the region next to the cold wall is not influenced by the heat source.

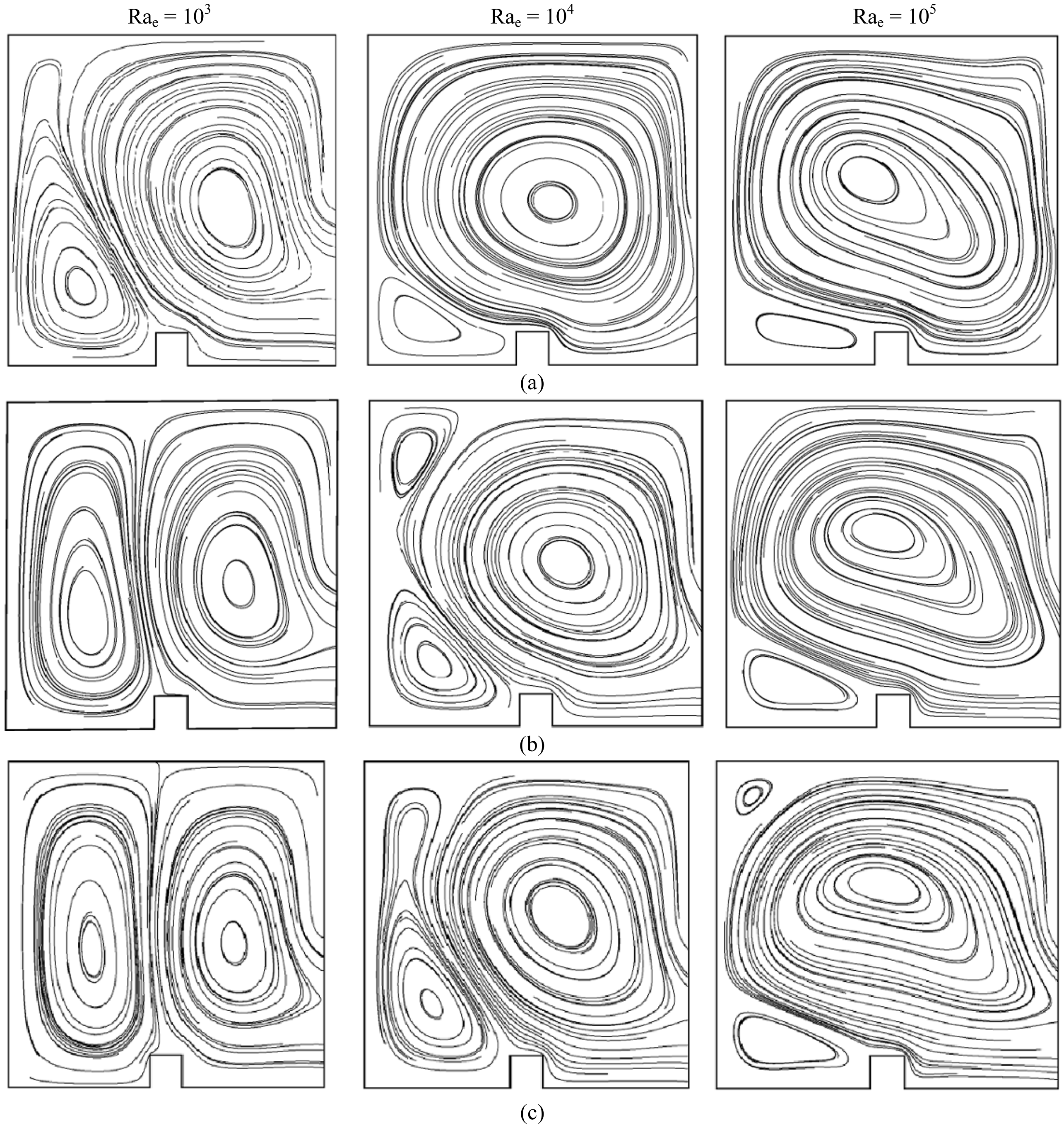

Figure 4: Streamlines for (a) R =400, (b) R = 1000, and (c) R = 2000.

When R = 2000, however, we find that for $Ra_e = 10^5$ it has the lowest values of local Nusselt while the maximum is reached when $Ra_e = 10^3$. In this case, the influence of the heat source becomes more evident, especially for small values of Ra_e, because in these cases the intensity of the recirculation is lower, so that the dissipation of heat generated by the source does not have great influence of the air fluid dynamic. So, the bottom next to the opening is more intensely heated, thereby increasing the gradient of temperature with the cold wall. For high values of Ra_e the intensity of main recirculation is greater, so that the distribution of temperature next to the cold wall does not have so much influence from the heat source.

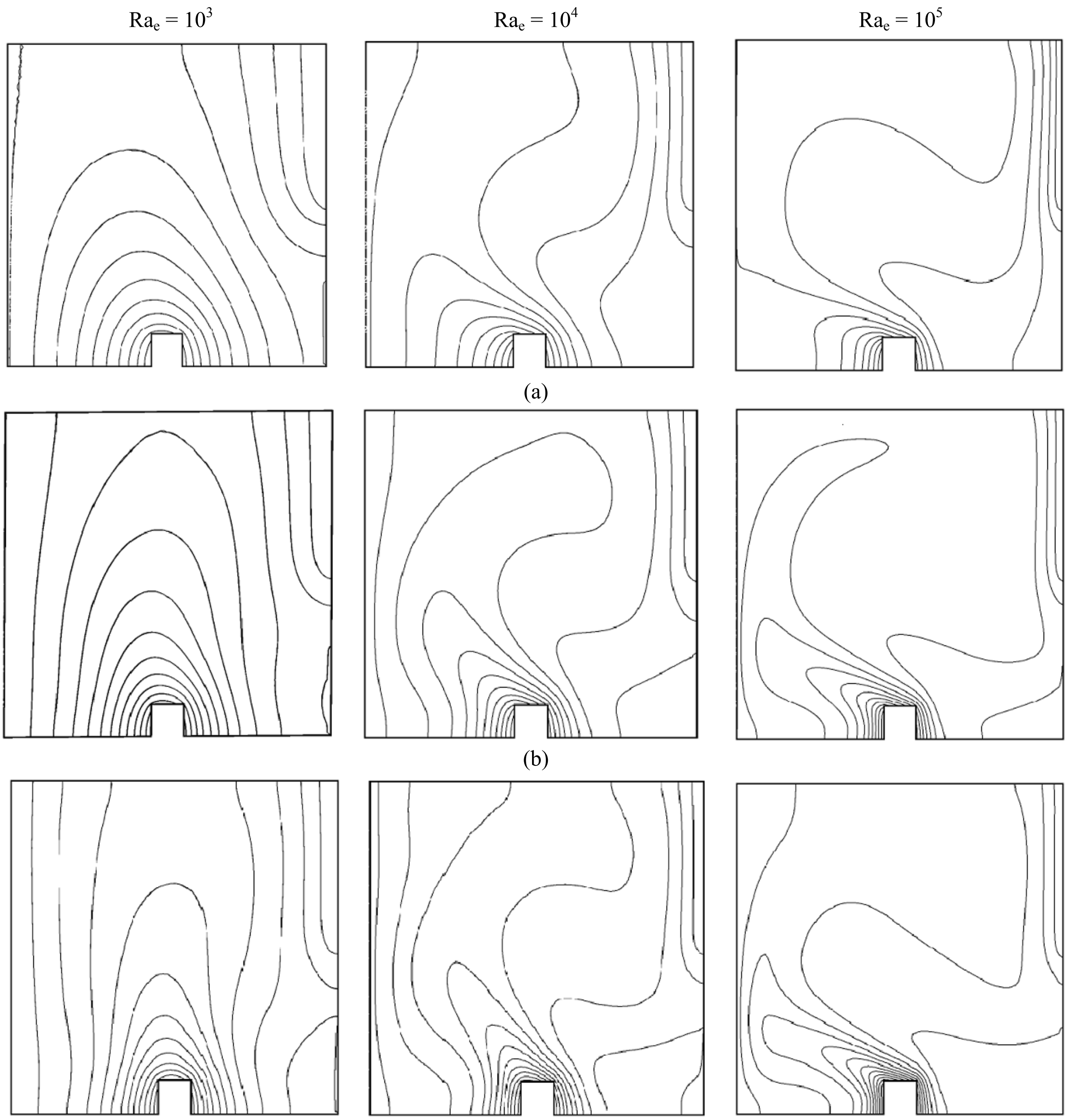

Figure 5: Isotherms for (a) R =400, (b) R = 1000, and (c) R = 2000.

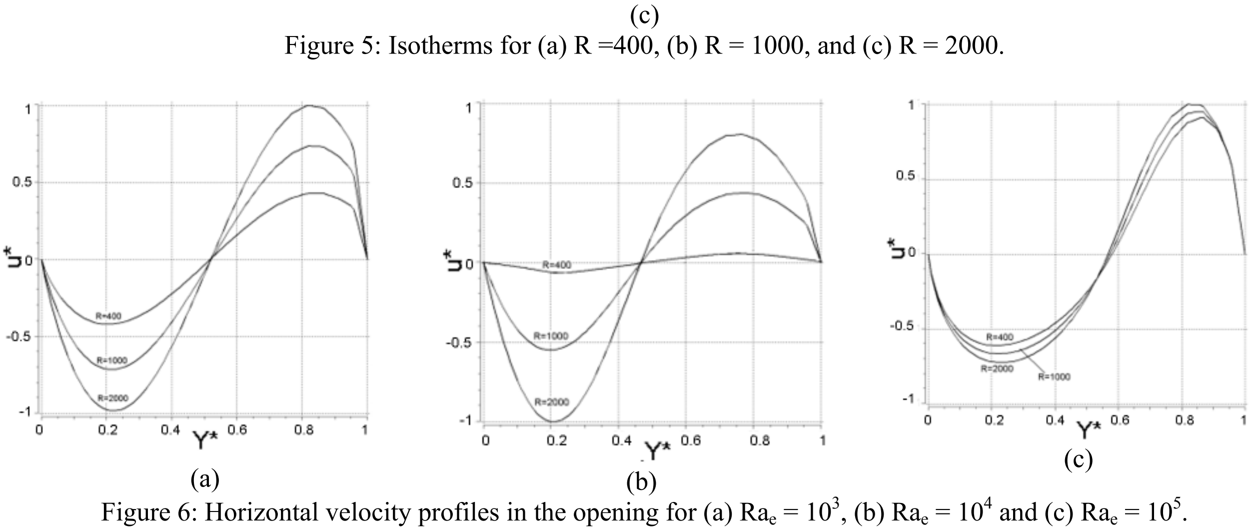

Figure 6: Horizontal velocity profiles in the opening for (a) $Ra_e = 10^3$, (b) $Ra_e = 10^4$ and (c) $Ra_e = 10^5$.

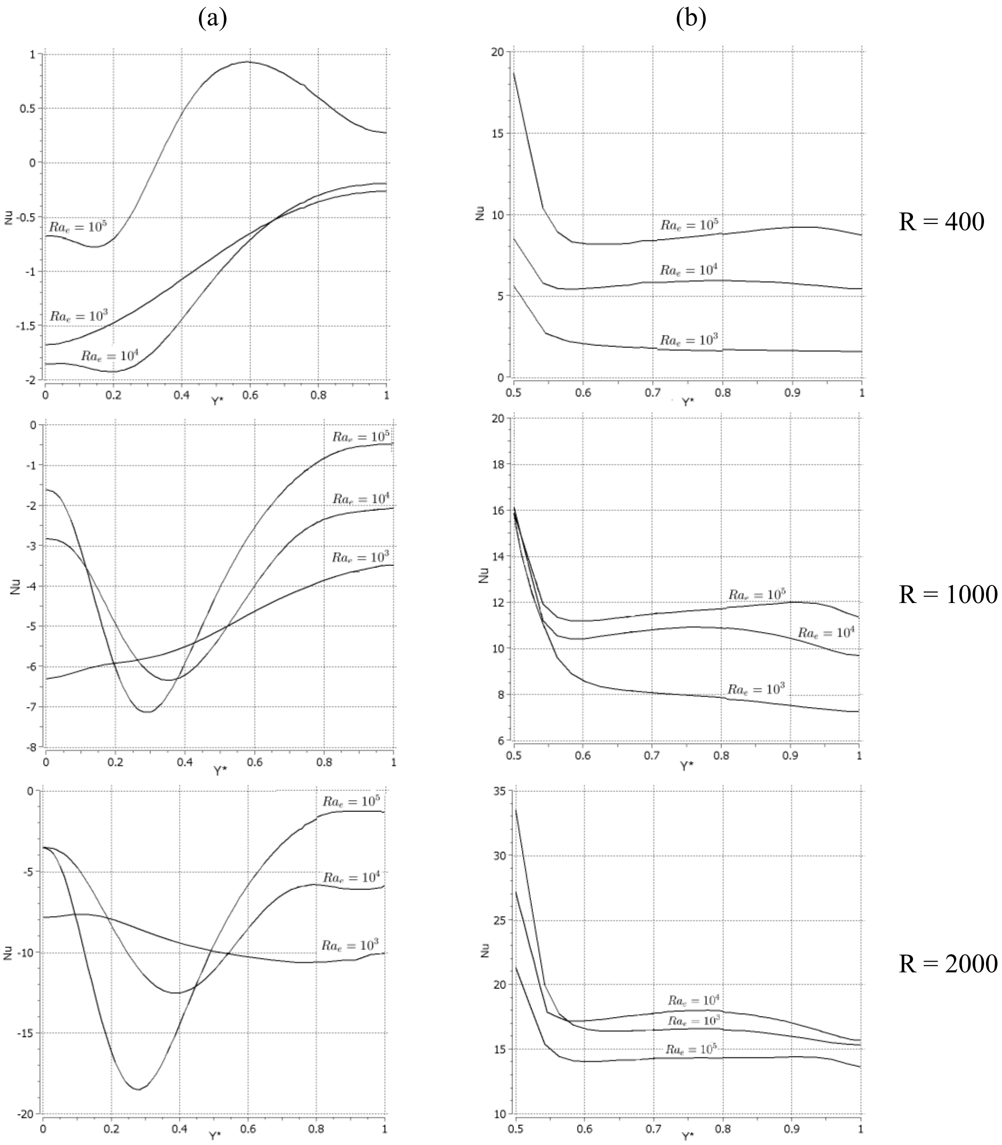

Figure 7: Local Nusselt number along the (a) hot and (b) cold walls versus Ra_e and R.

For local Nusselt along the hot wall, Figure 7a shows that when R = 400, for values of $Ra_e = 10^3$ and 10^4 the distribution of temperature in the region next to the hot wall is determined by the influence of heat source, as can be seen in Figure 5. Thus the temperature next to the wall is higher than the temperature of the wall, especially in the lower region of cavity. As the heat exchange occurs because the air provides heat to the hot wall, the value of local Nusselt is negative, the values of local Nusselt in module it is bigger in Y* = 0 and decreases as moves away from the source. For $Ra_e = 10^4$ there is a point of minimum for a value of $Y^* \neq 0$, caused by the presence of a recirculation. For R = 400 and $Ra_e = 10^5$ the values of local Nusselt along the hot wall have distinct characteristics and therefore in this case the influence of the heat source is much lower. The presence of the heat source in lower cavity makes the air temperature to be higher than the wall, causing negative local Nusselt numbers. The distribution of temperature in the upper cavity is controlled by inflow in cavity, so that for $Y^* \approx 0.35$ the value of local Nusselt becomes zero, then the wall and fluid are the same temperatures. The maximum is obtained for $Y^* \approx 0.6$ indicating the region where the air is at a lower temperature. From this point, the value of Nusselt tends to decrease due to heat supplied by the hot wall. For values of R = 1000 and R = 2000, the behavior of the curves for $Ra_e = 10^4$ and 10^5 is quite similar. Occurs the formation of a minimum point between Y* = 0.2 and 0.5, caused by the presence of a recirculation in the lower left of the cavity. After this region the value of Nusselt increases up to a constant value approximately close to Y* = 1, because in this region the influence of the heat source becomes gradually smaller.

5. CONCLUSIONS

The present study has investigated the variations of streamlines and isotherms as a function of different values of internal and external Rayleigh numbers, Ra_i and Ra_e, for square cavity. The cavity has an opening on the right wall and a small heating source located on the bottom vertical wall, occupying the central position. The phenomenon of natural convection was evaluated for values of Ra_e between 10^3 and 10^5, and R between 400 and 2000. The results show that the thermal and fluid dynamic behavior of the fluid is highly influenced by the presence of heat source, of the opening and of the temperature difference between the vertical walls. When the flow is controlled mainly by the heat source (high values of R and low values of Ra_e) there are large secondary circulations inside the cavity and the isotherms exhibit parabolic behavior, causing an increase (in modulus) in values of local Nusselt. When the natural convection is controlled by the temperature difference between the walls (low values of R and high values of Ra_e), the size of the secondary circulation is negligible from the main recirculation and the isotherms are more horizontal.

6. REFERENCES

Abourida, B., Hasnaoui, M., Douamma, S., 1998, "Natural Convection in a Square Cavity With Vertical Boundaries Submitted to Periodic Temperatures", Revue Generale de Thermique, Vol. 37, No. 9, pp. 788-800.

Barakos, G, Mitsoulis, E., Assimacopoulos, D., 2005, "Natural Convection Flow in a Square Cavity Revisted: Laminar and Turbulent Models with Walls Functions", International Journal for Numerical Methods in Fluid, Vol. 18, No. 7, pp. 695-719.

Bilen, E. e Oztop, H., 2005, "Natural Convection Heat Transfer in Partially Open Inclined Square Cavities", International Journal of Heat and Mass Transfer Vol. 48, pp. 1470-1479.

Costa, V. A. F., 2005, "Thermodynamic of Natural Convection in Enclosures with Viscous Dissipation", International Journal of Heat and Mass Transfer, Vol. 48, pp. 2333-2341.

Davis, G. V., 2005, "Natural Convection of Air in a Square Cavity: A Bench Mark Numerical Solution, International Journal for Numerical Methods in Fluids, Vol. 3 Iss. 3, pp. 249-264.

Hortmann, M., Peric, M., Scheuerer, G., 1990, "Finite Volume Multigrid Prediction of Laminar Natural Convection: Benchmark Solutions", International Journal of Methods in Fluids, Vol. 11, pp 189-207, 1990.

Kandaswamy, P., Lee, J. e Hakeem, A., 2007, "Natural Convection in a Square Cavity in the Presence of Heated Plate", Nonlinear Analysis: Modelling and Control, Vol. 12, No 2, pp. 203-212.

Kuznetsov, G. V. e Sheremet, M.A., 2009 ,"Conjugate heat transfer in an enclosure under the condition of internal mass transfer and in the presence of the local heat source". International Journal of Heat and Mass Transfer, Vol. 52, No 1-2, pp 1-8.

Kuznik, F, Vareilles, J., Rusaouen, G., Krauss, G., 2007, "A double-population lattice Boltzmann method with non-uniform mesh for the simulation of natural convection in a square cavity", Int. Journal of Heat and Fluid Flow, Vol. 28, pp. 862-870.

Maliska, C, 2004, "Transferência de Calor e Mecânica dos Fluidos Computacional", 2ª ed., LTC, Rio de Janeiro.

Mariani, V. C. e Silva, A., 2007, "Natural Convection: Analysis of Partially Open Enclosures with an Internal Heated Source", Numerical Heat Transfer, Part A, Vol. 52, pp. 595-619.

Mezrhab, A., Jami, M., Abid, C., Bouzidi, M., Lallemand, P., 2006, "Lattice-Boltzmann modelling of natural convection in an inclined square enclosure with partitions attached to its cold wall". International Journal of Heat and Fluid Flow, Vol 27, No. 3, pp. 456-465.

Michalek, T., 2005, "High Rayleigh Number Natural Convection in Cubic Enclosure", Proceeding of Eurotherm Seminar of Numerical Heat Transfer, Gliwice-Cracow, Poland.

Nakhi, A. B. e Chamkha, A. J., 2007, "Conjugate Natural Convection Arround a Finned Pipe in a Square Enclosure with Internal Heat Genereation", International Journal of Heat and Mass Transfer, Vol. 50, pp. 2260-2271.

Oztop, H. e Bilgen, E., 2006, "Natural Convection in Differentially Heated and Partially Divided Square Cavities with Internal Heat Generation", International Journal of Heat and Fluid Flow, Vol. 27, No.3, pp. 466-475.

Oztop, H. F. e Abu-Nada, E., 2008, "Numerical Study of Natural Convection in Partially Heated Rectangular Enclosures Filled with Nonofuids", International Journal of Heat and Fluid Flow, Vol. 29, No. 5, pp. 1326-1336.

Patankar, S. V., 1980, "Numerical Heat Transfer and Fluid Flow", Hemisphere Publishing Corporation.

Pesso, T. e Piva, S., 2009, "Laminar natural convection in a square cavity: Low Prandtl numbers and large density differences". International Journal of Heat and Mass Transfer, Vol 52, No 3-4, 31, pp. 1036-1043.

Sazia, A. A. Mohamad, 1999, "Suppressing free convection from a flat plate with poor conductor ribs", Int. J. Heat Mass Transfer, Vol. 42, pp. 2041-2051.

Xia, J. L. and Zhou, Z. W., 1992, "Natural Convection in an Externally Heated Partially Open Cavity with a Heated Protrusion", FED-vol. 143/HTD, Vol. 232, Measurement and Modeling of Environmental Flows – ASME, pp. 201-208.

Yilbas, B. S., Shuja, S. Z., Gradebo, S. A., Al-Hamayel, H. I. And Boran, K, 1998, Natural Convection and Entropy Generation in a Square Cavity, Int. J. of Energy Research, Vol. 22, pp. 1275-1290, 1998.

Zitzman, T, Cook, M, P. Pfrommer, S. Rees and L. Marjanovic, 2005, "Simulation of Steady State Natural Convection Using CFD", Proceeding of Building Simulation, Montreal, Canada.